

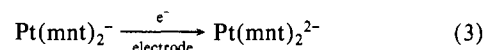
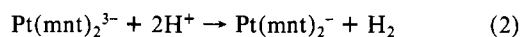
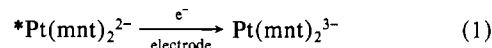
Figure 7. Absorption spectra of the electrode described in Figure 6 (a) before and (b) after irradiation.

Unfortunately, no luminescence evidence is available to decide the present case. The second possibility is that either neighboring complexes or, more probably, the π^* levels of the pyridine units of the backbone are available to act as electron-transfer partners with the excited state in the short time available before it decays. (An energy-transfer mechanism is less likely since excited-state lifetimes are so short in solution.^{1,4}) Whichever mechanism is responsible for the increase, the mobility of ionic species in the present films is not great and may limit efficiency. There is a requirement to transport anions in and out of the film as the charge on the complex changes, and the voltammograms of films are quite

- (2) Thomas, J. K.; Wheeler, J. J. *Photochemistry* **1985**, *28*, 285.
 (3) Kane-McGuire, N. A. P.; Clouts, G. M.; Kerr, R. C. *Inorg. Chim. Acta* **1980**, *44*, 457.
 (4) Persaud, L.; Sharma, D. K.; Langford, C. H. *Inorg. Chim. Acta* **1986**, *114*, L5.

sensitive to anions in the supporting electrolyte. We are now trying to extend work to ion-exchange polymer films in which ions are more mobile.

The Pt complexes behave similarly to those of Ni, with the quantitative difference that "recrystallization" on the film is more pronounced and the history of a film is more important. In addition, the development of the mixed-oxidation-state system produces an interesting heterogeneous electrocatalytic system for H_2 evolution at modest overpotentials. It is difficult to suggest just how the system may work. One possibility is



Two objections can be raised. First, the above cycle does not appear to need to wait for the "recrystallization" of the complex in the film into the solid particles "visible" to SEM, whereas the generation of H_2 is important only after some time of irradiation. Second, picosecond flash results reported recently⁴ indicate that the "triplet" excited state of $Pt(mnt)_2^{2-}$ is directly quenched by water in what is probably an electron-transfer step. Thus, the path is more complex. The steps shown in eq 1-3 may reflect, at best, a simplified monomolecular model for reactions occurring at the surface of mixed-oxidation-state microcrystalline particles. When solid $(R_4N)_2Pt(mnt)_2$ powders are dispersed in O_2 -free water and irradiated, they do undergo oxidation.

Acknowledgment. We thank the Natural Sciences and Engineering Research Council of Canada for financial support.

Registry No. $Ni(mnt)_2^{2-}$, 14876-79-0; $Pt(mnt)_2^{2-}$, 15152-99-5; SnO_2 , 18282-10-5; KCl, 7447-40-7; NaBr, 7647-15-6; NaCl, 7647-14-5; NaF, 7681-49-4; Pt, 7440-06-4; 4-vinylpyridine-styrene copolymer compound with benzyl chloride, 103564-34-7.

Contribution from the Department of Chemistry,
 Institut für Anorganische Chemie, D-6000 Frankfurt am Main 50, West Germany

Semireduced Bridging Ligands Containing $-N=N-$ Multiple Bond Coordination Sites. ESR Study of Binuclear Group 6 Metal Carbonyl Complexes

Wolfgang Kaim*† and Stephan Kohlmann

Received February 12, 1986

Centrosymmetric binuclear metal carbonyl complexes of anion radical ligands containing the azo group $-N=N-$ were studied by ESR. The ligands employed were 1,2,4,5-tetrazine (tz), 3,6-bis(2-pyridyl)-1,2,4,5-tetrazine (bptz), and azo-2,2'-bipyridine (abpy), and the following radical complexes were studied: $(\mu-(N^1, N^4)\text{-tz}^{\cdot-})[M(CO)_5]_2$ ($M = Mo, W$); $(\mu\text{-bptz}^{\cdot-})[M(CO)_4]_2$ and $(\mu\text{-abpy}^{\cdot-})[M(CO)_4]_2$ ($M = Cr, Mo, W$). The ESR spectra of abpy species are line rich and insufficiently resolved so that ENDOR spectroscopy was used in one case, viz., $(\mu\text{-abpy}^{\cdot-})[Mo(CO)_4]_2$. In contrast, the tetrazine complexes exhibit a rather simple ESR hyperfine structure because of spin localization at the four nitrogen centers in the tetrazine ring. The observed response of the hyperfine structure on metal coordination is well reproduced by HMO-McLachlan perturbation calculations of the spin distribution. Double coordination of equivalent metal fragments and spin localization at the tetrazine nitrogen centers create exceptionally favorable conditions to detect metal isotope coupling; a survey of these and several related anion radical complexes shows that the small metal isotope splittings are caused by σ/π spin polarization originating from the coordinating nitrogen π center.

Introduction

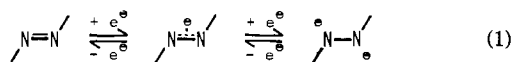
Compounds containing the azo group, $-N=N-$, such as azoalkanes, azoaromatics, or the cyclic conjugated 1,2,4,5-tetrazines are generally π -electron deficient;¹ they may be reduced at rather positive potentials² to form stable anion radicals³ or

dianions.^{2a,c} The nitrogen atoms in the azo linkage $-\bar{N}=\underline{N}-$ have unshared electron pairs available for coordination of electrophiles,

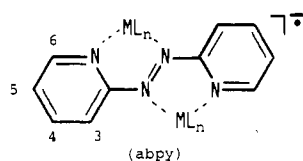
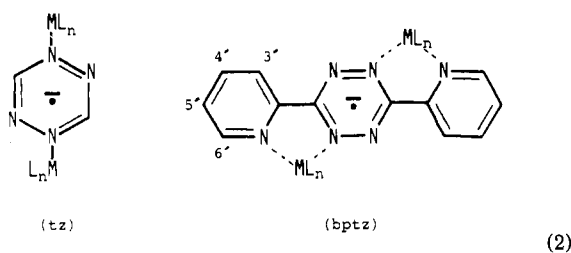
- (1) Modelli, A.; Jones, D.; Rossini, S.; DiStefano, G. *Tetrahedron* **1984**, *40*, 3257.
 (2) (a) Cheng, S.; Hawley, M. D. *J. Org. Chem.* **1985**, *50*, 3388 and literature cited therein. (b) Wiberg, K. B.; Lewis, T. P. *J. Am. Chem. Soc.* **1970**, *92*, 7154. (c) Troll, T. *Electrochim. Acta* **1982**, *27*, 1311. (d) Kaim, W. *J. Chem. Soc., Perkin Trans. 2* **1985**, 1633.

*Karl Winnacker Fellow, 1982-1987.

and although the very low basicity of these nitrogen centers⁴ renders azo compounds as relatively poor ligands, they can exhibit an extensive coordination chemistry.⁵ It has been known that such π acidic ligands can receive a very strong increase in their σ nucleophilicity upon reduction;⁶ anion radicals of α -diimine ligands such as 2,2'-bipyridine (bpy) or 1,10-phenanthroline have pK_{BH^+} values that are about 20 units higher than those of the neutral bases!^{6c} Accordingly, the semireduced forms of azo-containing compounds, i.e. their anion radicals, should constitute suitable ligands for metal electrophiles in a similar way as the final, fully reduced members in redox series 1.⁷



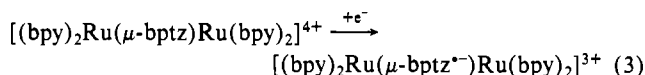
We present here an ESR study of several centrosymmetric binuclear radical complexes with bridging anion radical ligands containing the azo group, viz., pentacarbonylmolybdenum and -tungsten complexes of the 1,2,4,5-tetrazine anion radical $tz^{\cdot-}$ and tetracarbonylchromium, -molybdenum, and -tungsten complexes of the doubly bidentate anion radical of 3,6-bis(2-pyridyl)-1,2,4,5-tetrazine, $bptz^{\cdot-}$ (2). The ESR spectra of binuclear



tetracarbonylmol compounds with azo-2,2'-bipyridine anion radical (abpy $^{\cdot-}$) proved to be too complex for direct ESR analysis so that we had to resort to electron nuclear double resonance

(ENDOR)⁸ to obtain the ESR coupling constants of the molybdenum derivative. In addition to the ESR/ENDOR measurements, we have carried out π molecular orbital perturbation calculations at the Hückel/McLachlan level⁹ in order to assign the coupling constants and to understand their variation in different coordination compounds; such procedures had been successfully employed for a number of other anion radical coordination compounds of N-heterocyclic ligands.^{10,11}

Neutral complexes corresponding to the anion radical species presented here had been described before by Herberhold and Süss-Fink (pentacarbonylmetal systems)¹² and more recently by us (tetracarbonylmetal complexes).¹³ The neutral complexes are distinguished by very intense metal-to-ligand charge-transfer (MLCT, $\pi^* \leftarrow d$) absorption bands in the near-infrared red region, i.e. at extremely long wavelength; related to these unusual electron spectroscopic features are very positive reduction potentials around 0 V vs. a saturated calomel electrode (SCE).¹³ An investigation of the spin distribution in the singly reduced complexes should give some valuable information on the character of the π^* orbitals in the neutral species, i.e., on the MOs involved in the lowest MLCT transitions.^{10h,i} For example, we could recently present direct ESR evidence for localized reduction in a mixed poly-azine complex (3) of ruthenium(II) by using the $bptz$ ligand, which allowed us to record a fairly well-resolved ESR spectrum.¹⁴



Bridging ligands with very low lying π^* levels and electron delocalization are also of current interest as valuable electron-conducting components for low-dimensional coordination polymers;¹⁵ such materials may become good electrical conductors after the facile acquisition of extra electrons into the ligand π system. Recent results by Schneider and Hanack¹⁶ have demonstrated that the tetrazine bridge is a particularly promising component of such systems.

Experimental Section

The ligands tz ,¹⁷ $bptz$,¹⁸ and $abpy$ ¹⁹ and the binuclear complexes (μ - $bptz$)[Mo(CO)₄]₂, (μ - $bptz$)[W(CO)₄]₂, and (μ - $abpy$)[Mo(CO)₄]₂ were prepared as reported.¹³ Anion radicals for ESR measurements were generated under vacuum in sealed glass systems by reacting freshly distilled potassium either with dilute THF solutions of binuclear or mononuclear¹³ complexes or with mixtures of the free ligand and metal hexacarbonyl in THF (in situ complexation);²⁰ the latter method was

- (3) Azoalkane anion radicals: (a) Krynitzy, U.; Gerson, F.; Wiberg, N.; Veith, M. *Angew. Chem.* **1969**, *81*, 745; *Angew. Chem., Int. Ed. Engl.* **1969**, *8*, 755. (b) Sustmann, R.; Sauer, R. *J. Chem. Soc., Chem. Commun.* **1985**, 1248. Azoaromatic anion radicals: (c) Johnson, C. S.; Chang, R. *J. Chem. Phys.* **1965**, *43*, 3183. (d) Russell, G. A.; Konaka, R.; Strom, E. T.; Danen, W. C.; Chang, K.; Kaupp, G. *J. Am. Chem. Soc.* **1968**, *90*, 4646. (e) Neugebauer, F. A.; Weger, H. *Chem. Ber.* **1975**, *108*, 2703. Tetrazine anion radicals: (f) Stone, E. W.; Maki, A. H. *J. Chem. Phys.* **1963**, *39*, 1635. (g) Gerson, F.; Skorjanetz, W. *Helv. Chim. Acta* **1969**, *52*, 169. (h) Malkus, H.; Battiste, M. A.; White, R. M. *J. Chem. Soc., Chem. Commun.* **1970**, 479.
- (4) (a) $pK_a(\text{azobenzene-H}^+) = -2.48$; Klotz, I. M.; Fiess, H. A.; Chen Ho, J. Y.; Melody, M. *J. Am. Chem. Soc.* **1954**, *76*, 5136. (b) $pK_a(2\text{-phenylazopyridine-H}^+) = 2.0$; Foffani, A.; Foffani, M. *Atti. Accad. Naz. Lincei, Cl. Sci. Fis., Mat., Nat. Rend.* **1957**, *23*, 60; *Chem. Abstr.* **1959**, *53*, 824a. (c) $pK_a(1,2,4,5\text{-tetrazine-H}^+) \ll 0$; Spanget-Larsen, J. *J. Chem. Soc., Perkin Trans. 2* **1985**, 417. Cf. also: Mason, S. F. *J. Chem. Soc.* **1959**, 1247.
- (5) (a) Shunichiro, B.; Carter, D.; Fernando, Q. *J. Chem. Soc., Chem. Commun.* **1967**, 1301. (b) Albin, A.; Kisch, H. *Top. Curr. Chem.* **1976**, *65*, 105 and literature cited therein. (c) Frazier, C. C., III; Kisch, H. *Inorg. Chem.* **1978**, *17*, 2736. (d) Fochi, G.; Floriani, C.; Bart, J. C. J.; Giunchi, G. *J. Chem. Soc., Dalton Trans.* **1983**, 1515. (e) Albin, A.; Fasani, E. *J. Organomet. Chem.* **1984**, *273*, C26. (f) Datta, D.; Chakravorty, A. *Inorg. Chem.* **1983**, *22*, 1085. (g) Ghosh, B. K.; Mukhopadhyay, A.; Goswami, S.; Ray, S.; Chakravorty, A. *Ibid.* **1984**, *23*, 4633. (h) Herberhold, M.; Leonhard, K. *Angew. Chem., Int. Ed. Engl.* **1976**, *15*, 230.
- (6) (a) Ford, P.; Rudd, D. F. P.; Gaunder, R.; Taube, H. *J. Am. Chem. Soc.* **1968**, *90*, 1187. (b) Wiegardt, K.; Cohen, H.; Meyerstein, D. *Angew. Chem.* **1978**, *90*, 632; *Angew. Chem., Int. Ed. Engl.* **1978**, *17*, 608. (c) Krishnan, C. V.; Creutz, C.; Schwarz, H. A.; Sutin, N. *J. Am. Chem. Soc.* **1983**, *105*, 5617.
- (7) Henderson, R. A.; Leigh, G. J.; Pickett, C. J. *Adv. Inorg. Chem. Radiochem.* **1983**, *27*, 197.

- (8) Kurreck, H.; Kirste, B.; Lubitz, W. *Angew. Chem.* **1984**, *96*, 171; *Angew. Chem., Int. Ed. Engl.* **1984**, *23*, 173.
- (9) McLachlan, A. D. *Mol. Phys.* **1960**, *3*, 233.
- (10) (a) Kaim, W. *Chem. Ber.* **1981**, *114*, 3789. (b) Kaim, W. *J. Am. Chem. Soc.* **1982**, *104*, 3833, 7385. (c) Kaim, W. *J. Organomet. Chem.* **1983**, *241*, 157. (d) Kaim, W. *J. Am. Chem. Soc.* **1983**, *105*, 707. (e) Kaim, W. *J. Organomet. Chem.* **1984**, *264*, 317. (f) Kaim, W. *Inorg. Chem.* **1984**, *23*, 504. (g) Kaim, W. *Ibid.* **1984**, *23*, 3365. (h) Kaim, W. *Z. Naturforsch., B: Anorg. Chem. Org. Chem.* **1984**, *39B*, 801. (i) Kaim, W.; Ernst, S. *J. Phys. Chem.*, in press.
- (11) Application of the perturbation approach to phosphorus-containing anion radicals: (a) Kaim, W.; Hänel, P.; Bock, H. *Z. Naturforsch., B: Anorg. Chem., Org. Chem.* **1982**, *37b*, 1382. (b) Kaim, W.; Lechner-Knoblauch, U.; Hänel, P.; Bock, H. *J. Org. Chem.* **1983**, *48*, 4206.
- (12) Herberhold, M.; Süss-Fink, M. *Z. Naturforsch., B: Anorg. Chem., Org. Chem.* **1976**, *31B*, 1489.
- (13) (a) Kohlmann, S.; Ernst, S.; Kaim, W. *Angew. Chem.* **1985**, *97*, 698; *Angew. Chem., Int. Ed. Engl.* **1985**, *24*, 684. (b) Kohlmann, S.; Ernst, S.; Kaim, W. *Polyhedron* **1986**, *5*, 445. (c) Kohlmann, S.; Ernst, S.; Kaim, W., submitted for publication in *Inorg. Chem.*
- (14) Kaim, W.; Ernst, S.; Kohlmann, S.; Welkerling, P. *Chem. Phys. Lett.* **1985**, *118*, 431. Cf. also: Ernst, S.; Kaim, W. *Angew. Chem.* **1985**, *97*, 431; *Angew. Chem., Int. Ed. Engl.* **1985**, *24*, 430.
- (15) Hoffman, B. M.; Ibers, J. A. *Acc. Chem. Res.* **1983**, *16*, 15. Cf. also: *Chem. Eng. News* **1985**, 65 (Sept 30), 22.
- (16) Schneider, O.; Hanack, M. *Angew. Chem.* **1983**, *95*, 804; *Angew. Chem., Int. Ed. Engl.* **1983**, *22*, 784.
- (17) Curtius, T.; Darapsky, A.; Müller, E. *Ber. Dtsch. Chem. Ges.* **1907**, *40*, 815. Cf. also: Spencer, H. G.; Cross, P. C.; Wiberg, K. B. *J. Chem. Phys.* **1961**, *35*, 1939.
- (18) Geldard, J. F.; Lions, F. *J. Org. Chem.* **1965**, *30*, 318.
- (19) Kirpal, A.; Reiter, L. *Ber. Dtsch. Chem. Ges.* **1927**, *60*, 664. Cf. also: Baldwin, A.; Lever, A. B. P.; Parish, R. V. *Inorg. Chem.* **1969**, *8*, 107.

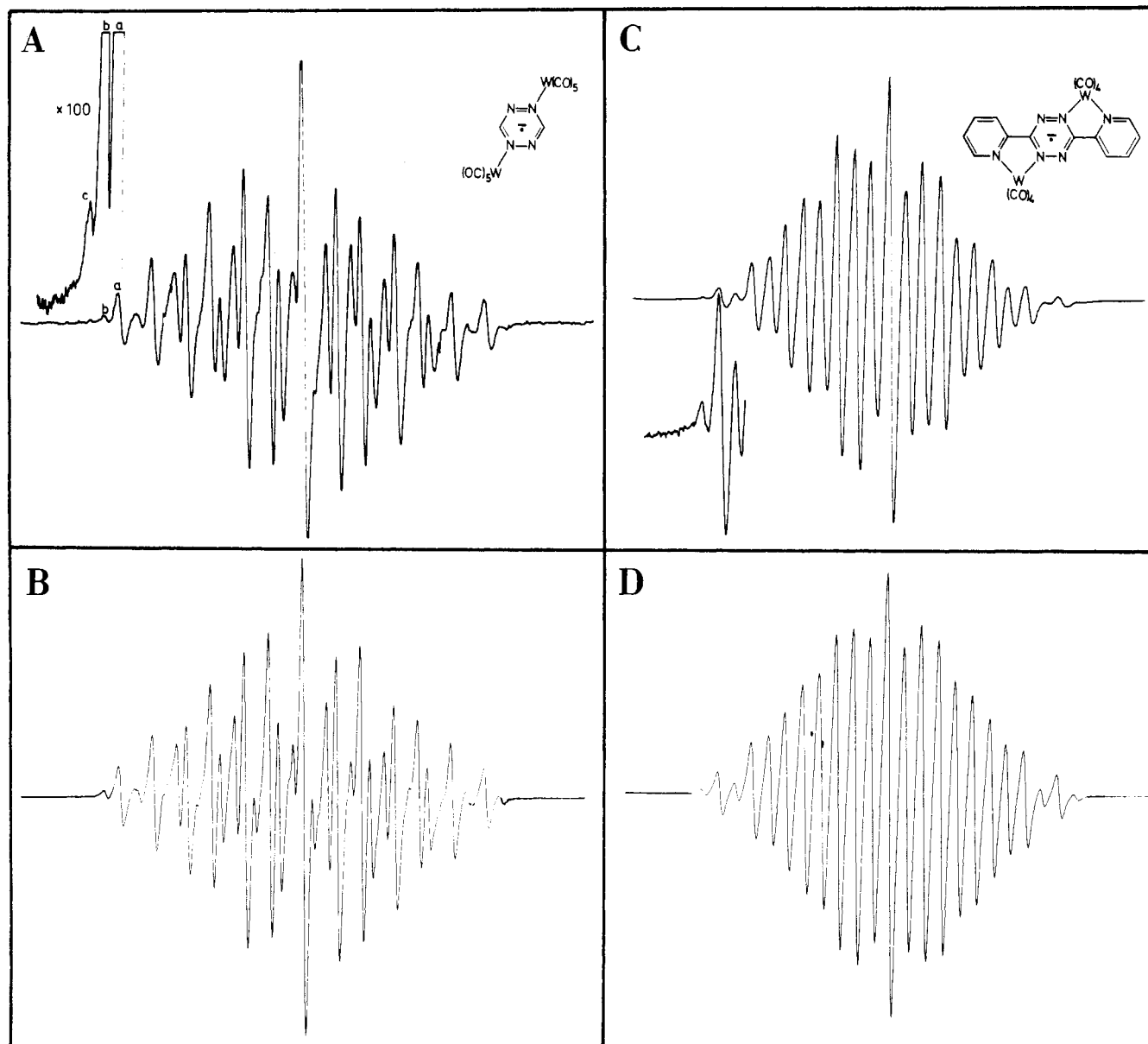


Figure 1. ESR spectra of $(\mu\text{-tz}^-)[\text{W}(\text{CO})_5]_2$ (A) and $(\mu\text{-bptz}^-)[\text{W}(\text{CO})_4]_2$ (C) at room temperature in THF solution, counterion K^+ . Amplified low-field wing sections reveal ^{183}W satellite lines; the letters in part A denote lines resulting from isotope combinations without ^{183}W nuclei (a), with one ^{183}W nucleus (b), and with two ^{183}W nuclei (c). Computer simulations (B, D) of the experimental spectra were obtained by using the data from Table I and line widths of 0.09 (B) and 0.10 mT (D), 25 theoretical lines (excluding metal isotope coupling).

employed to generate $(\mu\text{-tz}^-)[\text{Mo}(\text{CO})_5]_2$, $(\mu\text{-tz}^-)[\text{W}(\text{CO})_5]_2$, $(\mu\text{-bptz}^-)[\text{Cr}(\text{CO})_4]_2$, and $(\mu\text{-abpy}^-)[\text{W}(\text{CO})_4]_2$. $(\mu\text{-tz}^-)[\text{Cr}(\text{CO})_5]_2$ could not be obtained under these conditions. Most of the radical solutions thus prepared were persistent for several weeks at room temperature.

ESR spectra were recorded on a Varian E9 instrument in the X band (9.5 GHz). For calibration and g value determination by the double-cavity technique,^{10b} we used the perylene anion radical in 1,2-dimethoxyethane.²¹ The splitting patterns of the ESR spectra, including isotope satellite features, were analyzed with the help of computer simulations (Figure 1) using the program ESPLOT.^{10b} ENDOR spectra were taken on a Bruker ER 220 D LR instrument; we thank Dipl.-Chem. H. Herrmann and Prof. H. Bock for the measurements. HMO-McLachlan calculations⁹ ($k_{\text{CN}} = k_{\text{NN}} = 1.0$, $\gamma = 1.2$) and ESR simulations were performed on a VAX 750/11 system.

ESR/ENDOR Results

In agreement with the electrochemical studies, which showed reversible first reduction couples at unusually positive potentials in the cases of $(\mu\text{-bptz})[\text{Mo}(\text{CO})_4]_2$, $(\mu\text{-bptz})[\text{W}(\text{CO})_4]_2$, and

$(\mu\text{-abpy})[\text{Mo}(\text{CO})_4]_2$,¹³ the anion radicals of all the compounds investigated (2) proved to be persistent at room temperature under the conditions of ESR measurement (K^+ counterions, THF solutions). Formation of these binuclear anion radical complexes could be effected not only by e.g. alkali-metal or cobaltocene^{13c,22} reduction of the neutral binuclear complexes but also by reducing mononuclear species or mixtures that contain the hexacarbonylmetal and the free ligand in THF, i.e., by electron-transfer-activated carbonyl substitution.²⁰ The latter methods proved to be valuable in those instances when the neutral binuclear complexes were unstable or available only in very low yields; the formation of binuclear anion radical complexes by reduction of neutral mononuclear compounds seems to be a common phenomenon in the electron-transfer chemistry of coordination compounds.^{10e,23,29} The bis(pentacarbonylchromium) complex of the

(20) (a) Kaim, W. *Inorg. Chim. Acta* **1981**, 53, L151. (b) Kaim, W. *Chem. Ber.* **1982**, 115, 910.

(21) Bolton, J. R. *J. Phys. Chem.* **1967**, 71, 3702.

(22) Cf.: Becher, H. J.; Fenske, D.; Heymann, M. *Z. Anorg. Allg. Chem.* **1981**, 475, 27, or Dunbar, K. R.; Walton, R. A. *Inorg. Chem.* **1985**, 24, 5.

(23) Gross, R.; Kaim, W. *Inorg. Chem.* **1986**, 25, 498.

(24) Kaim, W.; Bock, H. *J. Organomet. Chem.* **1979**, 164, 281.

(25) Fenske, D.; Kohlmann, S.; Kaim, W., unpublished structural results.

Table I. Hyperfine Coupling Constants and g Values of Azo-Containing Anion Radicals and of Their Group 6 Metal Carbonyl Complexes^a

radical	$a_{N(\text{azo})}$	$a_{N'(\text{azo})}^b$	a_M^c	a_X	g
tz^{*-d}	0.528	0.528		0.021 ($\text{H}_{3,6}$)	e
$(\mu\text{-tz}^{*-})[\text{Mo}(\text{CO})_5]_2$	0.705	0.433	0.185	0.021 ($\text{H}_{3,6}$)	2.0047
$(\mu\text{-tz}^{*-})[\text{W}(\text{CO})_5]_2$	0.715	0.418	0.368	e	2.0070
bptz^{*-}	0.495	0.495		e	2.0040
$(\mu\text{-bptz}^{*-})[\text{Cr}(\text{CO})_4]_2$	0.622	0.459	0.11	e	2.0033
$(\mu\text{-bptz}^{*-})[\text{Mo}(\text{CO})_4]_2$	0.640	0.420	0.22	0.017 ($\text{H}_{3,5}$) ^f	2.0045
$(\mu\text{-bptz}^{*-})[\text{W}(\text{CO})_4]_2$	0.640	0.415	0.415	e	2.0068
abpy^{*-}	g	g	g	g	2.0044
$(\mu\text{-abpy}^{*-})[\text{Cr}(\text{CO})_4]_2$	g	g	g	g	2.0040
$(\mu\text{-abpy}^{*-})[\text{Mo}(\text{CO})_4]_2$	0.60 ^h	e		0.24 (N_1) ^f	2.0050
				0.186 (H_3)	
				0.00 (H_4)	
				0.255 (H_5)	
				0.054 (H_6)	
$(\mu\text{-abpy}^{*-})[\text{W}(\text{CO})_4]_2$	g	g	g	g	2.0089

^a Coupling constants a in mT (1 mT = 10 G = 28.0 MHz at $g = 2$). ESR measurements in THF solutions at ambient temperature, counterion K^+ . ^b N refers to coordinating, N' to non-coordinating azo centers in the complexes. ^c ⁵³Cr, 9.5% natural abundance, $I = 3/2$; ^{95,97}Mo, 15.8% and 9.6%, $I = 5/2$; ¹⁸³W, 14.3%, $I = 1/2$. ^d Reference 3f. ^e Not reported or observed. ^f From ENDOR measurements at 220 (¹H ENDOR) or 250 K (¹⁴N ENDOR). ^g Hyperfine splitting not analyzed by ESR. ^h Estimated from total ESR spectral width.

tetrazine anion radical could not be obtained via this route, in accordance with similar observations made on other N-heterocyclic anion radicals.^{20,23}

The ESR hyperfine structures (HFS) of the paramagnetic complexes discussed here may be divided into two categories. Anion radicals containing the 1,2,4,5-tetrazine group exhibit comparatively few lines in their ESR spectra (Figure 1); this splitting results from hyperfine interaction of the unpaired electron with the two different pairs of ¹⁴N nuclei in the symmetrically coordinating tetrazine ring and with metal isotopes of nonzero nuclear spin. The conditions necessary to observe metal isotope hyperfine splitting of nuclei in rather low natural abundance are exceptionally favorable in the centrosymmetric binuclear radical complexes of tetrazine anion radicals because of statistical reasons (two equivalent metal centers)^{10g} and because of the fact that these nuclei are coordinated to nitrogen centers with high π spin density.

For complexes such as $(\mu\text{-tz}^{*-})[\text{W}(\text{CO})_5]_2$, it has thus been possible to resolve ESR signals arising from species in which both metal atoms are present as spin-active nuclei (Figure 1A). A statistical treatment of this case yields probabilities of 0.74, 0.24, and 0.02 for the three combinations ¹⁸³W/¹⁸³W, ¹⁸³W/¹⁸³W, and ¹⁸³W/¹⁸³W, respectively;^{10g} x denotes an isotope without nuclear spin, and ¹⁸³W has $I = 1/2$ and 14.3% natural abundance. The actual line intensities observed are further reduced by the splitting pattern invoked.²⁴ For ¹⁸³W, one magnetically active nucleus gives rise to a 1:1 doublet splitting centered around the parent line, thus reducing the probability of each doublet component to $0.24/2 = 0.12$. Two equivalent ¹⁸³W centers result in a 1:2:1 triplet splitting which leaves a probability of only $0.02/4 = 0.005$ for each outer component. Compared with the parent line (100%; line a in Figure 1A), the relative intensities of the satellite lines are then 16% for the ¹⁸³W/¹⁸³W combination (line b in Figure 1A) and 0.7% for the ¹⁸³W/¹⁸³W combination (line c in Figure 1A); the observed ratios are in good agreement with these predictions from statistics.

Figure 1 illustrates that the two binuclear tungsten carbonyl complexes of tz^{*-} and bptz^{*-} display the same ESR splitting pattern

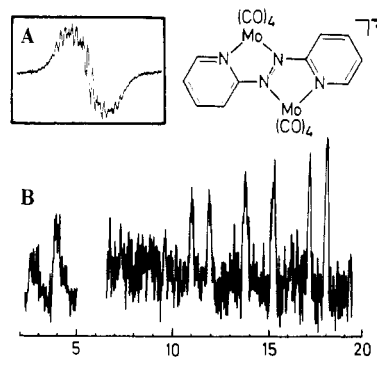


Figure 2. (A) ESR spectrum of $(\mu\text{-abpy}^{*-})[\text{Mo}(\text{CO})_4]_2$ under high-resolution conditions (room temperature, dilute THF solution). (B) Second-derivative ENDOR spectrum of the complex at 250 K (2–5 MHz) and 220 K (6–20 MHz). According to the ENDOR resonance condition, $\nu_{\text{ENDOR}} = |\nu_1 \pm a_1/2|$, ¹H lines are centered around the free proton frequency of $\nu_{\text{H}} = 14.6$ MHz and ¹⁴N resonances are centered around half of the coupling constant ($\nu_{^{14}\text{N}} = 1.05$ MHz at 0.33 T magnetic field).

arising from 2×2 equivalent ¹⁴N and 2 equivalent ¹⁸³W nuclei, albeit with significantly different coupling constants.

As concerns the splittings by the protons in tz^{*-} and bptz^{*-} complexes and the splittings of the pyridine ¹⁴N centers in bptz^{*-} species, these are expected to be rather small as a result of the MO nodal properties of tetrazines^{3f} (cf. MO calculations presented in the following section). Only for $(\mu\text{-tz}^{*-})[\text{Mo}(\text{CO})_5]_2$ could we detect a ¹H coupling constant of the same magnitude as that in the ligand anion tz^{*-} by ESR (Table I); broader lines of the tungsten analogue precluded observation of a_{H} . ENDOR spectroscopy had to be employed to obtain information on the spin density in the pyridyl rings of bptz^{*-} complexes, a single ¹H ENDOR line pair observed for $(\mu\text{-bptz}^{*-})[\text{Mo}(\text{CO})_4]_2$ yields a largest proton coupling constant of 0.017 mT.

The ESR hyperfine structure of abpy^{*-} and its complexes is very different. The ESR spectra are not sufficiently resolved due to considerable interaction of the unpaired electron with the nuclei in the pyridine rings; furthermore, the resulting number of 2025 theoretical lines for a C_{2h} symmetrical ligand (coordination-induced conformation in binuclear complexes²⁵) as well as the established tendency for anisotropic line-broadening in such anion radicals^{3c} led to ESR spectra that do not permit immediate hyperfine structure analyses (Figure 2A). We therefore resorted to ENDOR spectroscopy in one representative example, viz., $(\mu\text{-abpy}^{*-})[\text{Mo}(\text{CO})_4]_2$ (Figure 2B), from which one ¹⁴N and three ¹H splitting constants could be extracted. One proton splitting is apparently very small and, as the second ¹⁴N coupling, not detected by ENDOR. This latter result as well as estimations from the total ESR spectral width suggests that the large azo nitrogen coupling is in fact severely affected by anisotropic contributions to the $a_{^{14}\text{N}}$ and g tensors even at ambient temperature in fluid solution.^{3c}

Assignments of Coupling Constants

All binuclear radical complexes presented are centrosymmetric so that pairs of equivalent nuclei couple with the unpaired electron. Assignment of the observed coupling parameters (Table I) was aided by HMO-McLachlan perturbation calculations (Figure 3) and by the established fact that coordination of a carbonylmetal fragment alone causes an increase of the ¹⁴N coupling constant by about 0.1 mT relative to the value for the free ligand radical; both tetracarbonylmetal fragments in chelate position and pentacarbonylmetal fragments coordinating to peripheral nitrogen centers induce this increase.^{10e-1,20} Characteristic responses of the ¹⁴N HFS in heterocyclic anion radicals on coordination of organometallic fragments have been observed several times;^{10,20,23,26} the second-row main-group organometal fragments containing magnesium, aluminum, or silicon induce a lowering of $a_{^{14}\text{N}}$, whereas coordination of most other fragments, including transition metal carbonyl species, tends to cause a relative increase of $a_{^{14}\text{N}}$, quite independently of the overall π spin distribution change.

(26) Kaim, W. Z. *Naturforsch., B: Anorg. Chem., Org. Chem.* **1981**, *36B*, 677, 1110.

(27) Sullivan, P. D. *J. Am. Chem. Soc.* **1975**, *97*, 3992.

(28) Higuchi, J.; Ishizu, K.; Nemoto, F.; Tajima, K.; Suzuki, H.; Ogawa, K. *J. Am. Chem. Soc.* **1984**, *106*, 5403.

(29) For definition, cf.: Gross, R.; Kaim, W. *Angew. Chem.* **1985**, *97*, 869; *Angew. Chem., Int. Ed. Engl.* **1985**, *24*, 856. See also: Kaim, W. *Coord. Chem. Rev.*, in press.

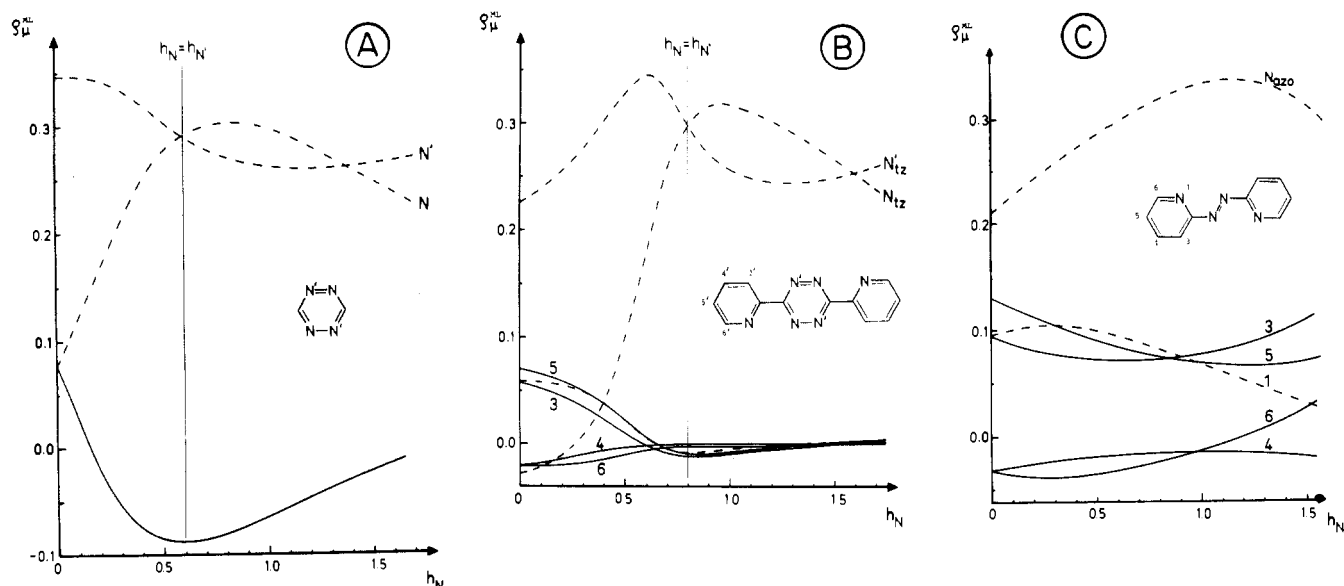


Figure 3. Perturbation diagrams showing calculated McLachlan spin densities ρ_{μ}^{ML} at various centers μ in binucleating anion radicals $\text{tz}^{\bullet-}$ (A), $\text{bptz}^{\bullet-}$ (B), and $\text{abpy}^{\bullet-}$ (C) as a function of the Coulomb integral parameter h_N . Noncoordinating centers N' have $h_{\text{N}'} = 0.6$ ($\text{tz}^{\bullet-}$) or $h_{\text{N}'} = 0.8$ ($\text{bptz}^{\bullet-}$), and the McLachlan parameter is $\lambda = 1.2$; broken lines refer to nitrogen centers.

In the perturbation procedure, the Coulomb integral parameter h_N of the coordinating (α -diimine) nitrogen centers serves as perturbation parameter (Figure 3). The noncoordinating N centers have $h_{\text{N}'} = 0.6$ ($\text{tz}^{\bullet-}$) or 0.8 ($\text{bptz}^{\bullet-}$) so that $h_N = h_{\text{N}'}$ should represent the situation for the free ligand anion radical; coordination of an electrophilic metal fragment is then reproduced by increasing the Coulomb integral at the coordination site.¹⁰ Such correlation diagrams have been advantageously used in previous studies to reproduce the effect of coordination of electrophiles on the experimental spin distribution of anion radical ligands; in addition, this approach also allows more reliable assignments of coupling constants than single parameter calculations of hyperfine splittings.¹⁰

The $\text{tz}^{\bullet-}$ and $\text{bptz}^{\bullet-}$ systems exhibit similar correlations between McLachlan spin populations ρ_{μ}^{ML} and h_N (Figure 3A,B). Starting from $h_N = h_{\text{N}'}$ (free ligand anion situation), the coordinating nitrogen centers should receive more spin density than the noncoordinating centers until this situation is reversed at very high h_N values. The larger ^{14}N coupling constant in the $\text{tz}^{\bullet-}$ and $\text{bptz}^{\bullet-}$ complexes can thus be confidently assigned to the coordinating nitrogen atoms of the tetrazine ring. In contrast to these very large π densities at the tetrazine nitrogen centers, the spin population at the 3,6-positions is small and often negative because of the nodal properties of the six-membered ring π system.^{3f,27} This affects not only the parent species $\text{tz}^{\bullet-}$ but also the various centers in the pyridyl rings of $\text{bptz}^{\bullet-}$ (Figure 3B), thus reflecting the superior electron-acceptor function of tetrazine relative to pyridine. In the relevant region $h_N > h_{\text{N}'}$ these spin populations ρ_{μ}^{ML} converge to zero; however, a slight remaining spin delocalization into the pyridyl rings is experimentally evident from the small reduction of the coupling constant for the tetrazine nitrogens in the ligand anion radical $\text{bptz}^{\bullet-}$ relative to that in $\text{tz}^{\bullet-}$ (Table I). The only ^1H coupling detected by ENDOR for $(\mu\text{-bptz}^{\bullet-})\text{[Mo(CO)}_4\text{]}_2$ is tentatively assigned to the protons in positions 3' and/or 5' of the pyridine rings.

In the $\text{abpy}^{\bullet-}$ complexes, on the other hand, the azo group is not as powerful in localizing the spin as in the tetrazine systems (Figure 3C). Although the McLachlan spin populations at the azo nitrogen centers are clearly very large, there is still significant delocalization to the various π centers in the pyridine rings. By using a Coulomb parameter of $h_N \approx 0.5$, one obtains a sequence of spin populations $\rho^{\text{ML}}(5) > \rho^{\text{ML}}(3) > \rho^{\text{ML}}(4) > \rho^{\text{ML}}(6)$, which is in agreement with assignments made for related 14-center/15- π -electron radicals such as *trans*-azobenzenes^{3e} or *trans*-stilbenes.²⁸ However, the actual proton coupling constants for $(\mu\text{-abpy}^{\bullet-})\text{[Mo(CO)}_4\text{]}_2$ as obtained by ENDOR (Table I) are

somewhat ($\sim 1/3$) lower than those of azobenzene or stilbene anion radicals, reflecting the transfer of spin to the metal-coordinating nitrogen centers. While ENDOR spectroscopy has allowed us to determine the smaller ^{14}N coupling in $(\mu\text{-abpy}^{\bullet-})\text{[Mo(CO)}_4\text{]}_2$, signals from the azo nitrogen centers could not be observed either as resolved ESR components or as ENDOR line pairs; the well-known large anisotropic contributions associated with ^{14}N -(azo) splittings^{3c} are probably responsible for these effects. Nevertheless, a rough estimate of $a^{14}\text{N}(\text{azo})$ was made on the basis of computer simulations of the total ESR spectral width.

Discussion

Spin Distribution. The ESR data of radical ligands and complexes in Table I clearly indicate the radical complex nature²⁹ of these paramagnetic coordination compounds; the spin is almost exclusively confined to the heterocyclic π system. This result lends additional evidence to the assignments of the intense and extremely long wavelength absorption bands of the neutral complexes as MLCT ($\pi^* \leftarrow d$) transitions.¹³ Whereas the abpy systems exhibit some delocalization (about 40%) of spin into the 2-pyridyl rings, this delocalization is almost negligible in the bptz anion radical complexes, the unpaired electron being virtually confined to the four azo nitrogen centers. The spin localization in the tetrazine-containing radical complexes is in agreement with the calculated spin distribution; it leads to ESR spectra with comparatively few lines and large coupling constants, thus creating very favorable conditions for the detection of metal isotope hyperfine splittings (Figure 1A).

A characteristic feature of the tetrazine complexes is the nonequivalence of the four nitrogen centers; one pair has a larger ^{14}N coupling constant (coordinating centers) and the other pair has a smaller nitrogen hyperfine splitting than in the corresponding free ligand anion radical. Although this behavior is displayed both by the binuclear pentacarbonylmetal complexes of $\text{tz}^{\bullet-}$ and by the binuclear tetracarbonylmetal complexes of $\text{bptz}^{\bullet-}$, the difference between the two ^{14}N coupling constants is somewhat larger in the former case, possibly because the supporting pyridyl groups reduce the polarizing effect by the transition-metal fragment. The ESR spectra of the two tungsten complexes illustrate the resulting spectral differences (Figure 1A,C).

The spin distribution in $(\mu\text{-abpy}^{\bullet-})\text{[Mo(CO)}_4\text{]}_2$ as determined by ENDOR (Figure 2B) is qualitatively similar to that found in the analogous *trans*-azobenzene³ and *trans*-stilbene anion radicals,²⁸ albeit in a somewhat modified form. The reduction of spin density at the carbon π centers is in agreement with the perturbation diagram (Figure 3C), which predicts decreasing spin de-

localization to those centers with increasing h_N values (stilbene: $h_N = 0.0$). The difficulties encountered in observing the ^{14}N (azo) splitting by either ESR or ENDOR are not unexpected in view of the previous experience with this kind of anion radicals.^{3c} Anisotropic line broadening results from insufficient averaging of anisotropic g and HFS tensor components due to relatively slow motion in solution, an effect that can become particularly large for species which have a high moment of inertia³⁰ such as binuclear metal complexes¹⁰ⁱ and that strongly affects the coupling from those centers that have high spin densities and pronouncedly anisotropic g and HFS characteristics.^{31a}

Metal Isotope Coupling. The most conspicuous features in the ESR spectra of tetrazine radical complexes are the metal isotope satellite lines. The conditions to detect such spectral features are particularly favorable in these systems because (1) there are two equivalent metal coordination sites available which cause high satellite line intensities in binuclear complexes for statistical reasons (cf. previous sections),^{10g} (2) the ESR spectra have comparatively few, widely spaced lines resulting from ^{14}N splitting, and (3) the spin density at the coordinating nitrogen centers is high due to the localization of spin at only four π centers.

The translation of nitrogen π spin density ρ_N into metal isotope coupling a_M is assumed to occur via σ/π spin polarization as in hydrocarbon π radicals,³² leading to a McConnell-type equation (eq 4) where Q_{NM} is a constant. The nitrogen spin density ρ_N ,

$$a_M = Q_{NM}\rho_N \quad (4)$$

on the other hand, is related to the observable coupling constant a_N by the Karplus-Fraenkel equation (eq 5),³³ where X refers to

$$a_N = Q_N\rho_N + \sum Q_{NX}\rho_X \quad (5)$$

the neighboring centers of the nitrogen atom. Combination of (4) and (5) leads to a relation (eq 6) between the observable parameters a_M and a_N .

$$a_M = Q_{NM}/Q_M(a_N - \sum Q_{NX}\rho_X) \quad (6)$$

Fortunately, Q_{NX} is rather small for $X = \text{C}^{31b,33}$ so that a direct proportionality should result between a_M and a_N in radical complexes where the coordinating nitrogen centers have carbon atoms as the only neighbors; two diagrams (Figure 4) for penta- and tetracarboxymetal complexes with nitrogen-containing anion radicals demonstrate the validity of this assumption.

In the pentacarboxymetal series, there is satisfactory linear behavior of a_M vs. a_N as long as only ligands with two carbon atoms adjacent to the coordinating nitrogen centers are concerned. The parameters of linear correlations $a_M = ka_N + B$ are as follows: $k = 0.081$, $B = 0.000$, correlation coefficient $r = 0.999$ for chromium (^{53}Cr : 9.5% natural abundance, nuclear spin $I = 3/2$); $k = 0.172$, $B = 0.007$, $r = 0.987$ for molybdenum ($^{95,97}\text{Mo}$: 15.8% and 9.6%, $I = 5/2$), and $k = 0.333$, $B = 0.013$, $r = 0.989$ for tungsten pentacarboxymetal complexes (^{183}W : 14.3%, $I = 1/2$). A similarly good correlation is obtained for tetracarboxymolybdenum chelate complexes of nitrogen-containing anion radicals with $k = 0.418$, $B = 0.010$, and $r = 0.994$; there are not enough data available for tetracarboxylchromium and -tungsten complexes (Figure 4).

In those cases where other than carbon atoms are neighbors of the coordinating nitrogen center, the data points (in brackets) lie off the straight lines passing through the origin (Figure 4); the term $\sum Q_{NX}\rho_X$ is apparently no longer negligible in those instances. Figure 4 shows that the complexes with oxygen, sulfur, or selenium centers adjacent to the nitrogen atoms on one side^{10c,36}

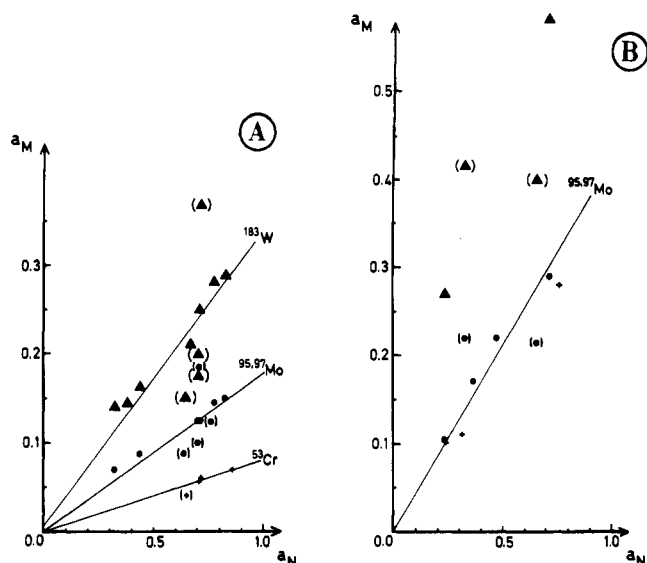


Figure 4. Correlation diagrams between metal isotope ESR coupling constants (in mT) and ^{14}N hyperfine splittings of the coordinating nitrogen centers in various anion radical complexes of group 6 metal pentacarboxymetal (A) and tetracarboxymetal (B) complexes. Crosses refer to chromium, filled circles to molybdenum, and filled triangles to tungsten complexes; the data involve the following ligands (as anion radicals): μ -pyrazine,²⁰ μ -2,5-dimethylpyrazine,^{20b} μ -quinoxaline,^{20b} μ -4,4'-bipyridine,²⁰ μ -bis(4-pyridyl)ethene,^{20b} μ -2,1,3-benzoxa(-thia-, -seleno-)diazoles,^{10c} 4-cyanopyridine- N^1 ,^{10f} μ -4,4'-bipyrimidine- $N^1, N^{1'}$,¹⁰ⁱ and (μ -)1,2,4,5-tetrazine for the pentacarboxymetal fragments (A) and μ -2,2'-bipyrimidine,^{10g} 2,2'-bipyridine,³⁴ glyoxal bis(*tert*-butylimine),³⁵ sulfur bis(*tert*-butylimide),³⁶ 2,2'-bipyrazine,¹⁰ⁱ and μ -3,6-bis(2-pyridyl)-1,2,4,5-tetrazine for the tetracarboxymetal fragments (B). Data points in brackets refer to anion radical complexes in which the coordinating nitrogen atoms have neighbors other than carbon atoms; straight lines were calculated by using only data points without brackets.

and the tetrazine complexes (which have -N-N- bonds) on the other side exhibit opposite deviation from the straight lines; the former exhibit rather small and the latter comparatively large metal hyperfine splitting in relation to the ^{14}N coupling constants of the coordinating centers.

Since bptz chelate complexes have nonequivalent metal coordination sites, we used average coupling constants \bar{a}_N in the diagram (Fig. 4B); the very small pyridine nitrogen coupling was neglected to yield $\bar{a}_N = a_{N(\text{azo})}/2$. When the metal isotope splittings of penta- and tetracarboxymetal radical complexes are compared, the double coordination (and double spin polarization) in the latter systems has to be taken into account by employing the squared sum of MO coefficients³⁷ or the effective π spin density ρ_{eff} for symmetrically chelated metal centers (ρ_0 : spin density at one coordination center).

$$\rho_{\text{eff}} = (2(\rho_0)^{1/2})^2 = 4\rho_0 \quad (7)$$

However, the ratio of k values for the molybdenum species is only $0.418/0.172 = 2.43$ and is thus significantly smaller than 4, perhaps reflecting structural restraints as imposed by the chelate situation. Conversely, a direct comparison of metal isotope hyperfine splittings in corresponding $\text{tz}^{\cdot-}$ and $\text{bptz}^{\cdot-}$ complexes shows larger values for the chelate complexes despite higher ^{14}N coupling constants of the $\text{tz}^{\cdot-}$ species; for an explanation of this divergence one has to consider the small contribution from the pyridyl π system and the more rigid conformation in the $\text{bptz}^{\cdot-}$ chelate complexes as well as the lowering of unoccupied metal-centered orbitals on replacement of a carbonyl ligand by a weaker π acceptor.¹⁰ⁱ

g Values. Previous studies have demonstrated that the isotropic g values of radical ion complexes are a very useful source of

(30) Kaim, W. Z. *Naturforsch., B: Anorg. Chem., Org. Chem.* **1981**, *36B*, 150.

(31) Gerson, F. *High Resolution E.S.R. Spectroscopy*; Wiley-Verlag Chemie: Weinheim, FRG, 1970: (a) pp 66-72; (b) pp 85-92.

(32) McConnell, H. M. *J. Chem. Phys.* **1956**, *24*, 632.

(33) Karplus, M.; Fraenkel, G. K. *J. Chem. Phys.* **1961**, *35*, 1312.

(34) tom Dieck, H.; Franz, K. D.; Hohmann, F. *Chem. Ber.* **1975**, *108*, 163.

(35) Franz, K. D.; tom Dieck, H.; Krynitz, U.; Renk, I. W. *J. Organomet. Chem.* **1974**, *64*, 361.

(36) Hunter, J. A.; King, B.; Lindsell, W. E.; Neish, M. A. *J. Chem. Soc., Dalton Trans.* **1980**, 880.

(37) Whiffen, D. H. *Mol. Phys.* **1963**, *6*, 223. For other applications of eq 7, cf.: Kaim, W.; Bock, H. *Chem. Ber.* **1978**, *111*, 3585; *J. Am. Chem. Soc.* **1980**, *102*, 4429.

